Kafkas Universitesi Veteriner Fakultesi Dergisi
Journal Home-Page: http://vetdergikafkas.org
E-ISSN: 1309-2251

Kafkas Univ Vet Fak Derg
31 (5): 661-667, 2025
DOI: 10.9775/kvfd.2025.34593

Research Article

Component Identification of Buyang Huanwu Decoction and the Effect of Main Components on Preventing Muscle Atrophy

Lan ZHOU [1] Shu LUO [1] Linglian MENG [1] Guangyao WANG [1] Lijing ZHANG [1] Haoxin WU [1] (*)

[1] College of Traditional Chinese Medicine, Nanjing University of Chinese Medicine, 210023 Nanjing, CHINA

(*) **Corresponding author:** Haoxin WU
Phone: +86-25-85389102
E-mail: 290366@njucm.edu.cn

How to cite this article?

Zhou L, Luo S, Meng L, Wang G, Zhang L, Wu H: Component identification of BYHWD and the effect of main components on preventing muscle atrophy. *Kafkas Univ Vet Fak Derg,* 31 (5): 661-667, 2025.
DOI: 10.9775/kvfd.2025.34593

Article ID: KVFD-2025-34593
Received: 04.06.2025
Accepted: 22.08.2025
Published Online: 15.09.2025

Abstract

Buyang Huanwu Dcoction (BYHWD) is a traditional Chinese medicine that has been widely used for the clinical treatment of skeletal muscle atrophy which is a common complication after motor neuron injury and seriously affects the recovery of skeletal muscle function. This study aimed to explore the main components of Buyang Huanwu decoction and its possible mechanism for treating skeletal muscle and nerve atrophy in mice. Total fibular nerve injury model was established by using total fibular nerve clamp surgery. Main component of decoction was detected by HPLC and LC-MS, the morphology of skeletal muscle samples was observed using hematoxylin-eosin staining (H&E) and laser lens, and the expressions of muscular atrophy related proteins were detected by Western blot. Astragaloside is the main components of BYHWD, it promotes the recovery of injured neuroskeletal muscle and significantly inhibits the atrophy of related muscle tissue ($P<0.05$). Denervation of skeletal muscle is closely related to autophagy, and Astragaloside can effectively inhibit autophagy after skeletal muscle injury. Astragaloside, the main component of BYHWD, promotes the recovery of skeletal muscle denervation by inhibiting autophagy.

Keywords: Astragaloside, Autophagy, Buyang Huanwu Decoction, Motor neuron injury, Neurogenic atrophy

Introduction

Muscle is a plastic tissue that continuously adjusts its shape, size, and function according to internal and external stimuli [1]. Local muscle atrophy is divided into disuse atrophy and denervation atrophy. Disuse atrophy often occurs in patients who are bedridden for a long time, or in patients with joint breaking for a long time, while denervation atrophy is mainly caused by neurological diseases or traumatic violence that damages skeletal muscle nerves [2]. Trauma or inflammation makes the nerves at the injury site undernourished, and the related skeletal muscles receive nerve impulses restricted, which in turn causes related muscle atrophy [3]. Compared with disuse atrophy, skeletal muscle denervation atrophy is more serious, and its treatment has always been the main focus of relevant clinical workers [4]. At present, the treatment of muscle atrophy is mostly limited to physical rehabilitation training and the treatment of a small number of hormone drugs. Therefore, an in-depth exploration of the pathogenic mechanism of muscle atrophy is crucial for taking targeted interventions, paying off muscle function, and improving the quality of the patient's life [5].

BYHW Decoction is a traditional prescription of traditional Chinese medicine. BYHWD is often used to treat the sequelae of cerebrovascular accidents (such as stroke), including facial paralysis, aphasia, hemiplegia, paraplegia and other diseases of Qi deficiency and blood stasis [6]. Nowadays, it is mostly used to treat neurological injury-related diseases such as cerebrovascular disease, facial nerve palsy, polio sequelae, sciatica, concussion sequelae, etc., and has achieved remarkable clinical effects [7].

In this study, we mainly analyzed the main pharmacological components of BYHWD, and studied the inhibitory effect of its main components on denervation of tibial anterior muscle in mice with peroneal nerve injury through animal experiments.

Material and Methods

Ethical Approval

All procedures performed involving animals were in accordance with the ethical standards of the Institutional Animal Care and Use Committee (IACUC) of Nanjing University of Chinese Medicine (No. 202203A041).

This article is licensed under a Creative Commons Attribution-NonCommercial 4.0 International License (CC BY-NC 4.0)

Animals

SPF grade, male, 6 weeks old, body weight 200 ± 10 g, 42 SD rats, purchased from Changzhou Cavens Laboratory Animal Co., Ltd. Laboratory animal license number: SCXK (Su) 2016-0010. All experimental animals began formal experiments after one week of adaptive feeding.

Animal Model

Rats were weighed, 10% chloral hydrate (300 g/mL) was injected intraperitoneally for anesthesia, and the surgical area of the left femur was routinely prepared and disinfected. Take a 1.5 cm incision in the middle of the left posterior femur, cut the skin and fascia in turn, free and fully expose the femur of the sciatic nerve, and perform the common peroneal nerve clamp down. With 14 cm hemostatic forceps, the upper total teeth clamp the common peroneal nerve 3 times, 10 seconds/time, 10 sec apart each time; the width of the crush injury is 5 mm. The distal end of the injury was marked with 9-0 non-invasive sutures, and the surgical incision was sutured layer by layer. After the rats woke up, they were put back into the cage for normal feeding. All animals were injected with the corresponding drug intraperitoneally on the 2nd day after modeling, and the normal group and the model group were injected with the same amount of normal saline for 7 days. After 18 days of surgical modeling, all rats were euthanized, and the tibial anterior muscle tissues on the left and right sides of the rats were taken respectively. The tibial anterior muscle tissue was divided into three parts for storage: 2.5% glutaraldehyde solution was fixed at 4°C; -80°C was stored at low temperature; 4% paraformaldehyde solution was fixed at room temperature for subsequent detection.

Experimental Grouping

The first part of the experiment: Normal group (replaced by the right healthy side of the model group); (2) Model group; (3) Astragaloside group (20 mg/kg); (4) Capillary isoflavone group (20 mg/kg); (5) Ferulic acid group (100 mg/kg); (6) Paeoniflorin group (20 mg/kg); (7) Ligustrazine group (100 mg/kg); (8) Mecobalamine positive control group (600 μg/kg), 6 in each group. Intraperitoneal injection was started two days after modeling and lasted for a total of 7 days.

The second part of the experiment: Base on the first experiment, the main active ingredient group + FOXO agonist was added, and 40 mg/kg of FOXO agonist was injected intraperitoneally every day for 7 consecutive days. Intraperitoneal injection was started two days after modeling, which lasted for a total of 7 days. The normal group and the model group were injected with the same amount of normal saline.

HPLC and LC-MS Experiments

HPLC: Precisely weigh 0.55 mg of pilus isoflavones, ferulic acid, paeoniflorin, and ligustrazine samples, place them in 10 mL brown volumetric flasks, add 70% methanol solution to dissolve and dilute to scale, and make a sample containing 0.055 mg per mL. Reference solution. Precisely weigh Buyang Huanwu Decoction and add methanol to dissolve, centrifuge the supernatant, and put the bandwidth evaluation in a 5 mL volumetric flask, shake well, and get it. Detection conditions: mobile phase: A 0.05% H_3PO_4 aqueous solution; B 0.1% methanol; chromatographic column: Symmetry C18, 4.6 x 250 mm; flow rate: 0.6 mL/min; column temperature: 30°C; injection volume: 5 μL; DAD detector Detection wavelength: 320 nm.

LC-MS: Take 0.0050 g of Astragaloside reference substance, weigh it precisely, place it in a 10 mL volumetric flask, add an appropriate amount of methanol to dissolve and dilute to scale, and make a solution containing 0.5 mg per 1 mL. Precisely weigh BYHW Decoction and add methanol to dissolve, centrifuge the supernatant, and put the bandwidth evaluation in a 5 mL volumetric flask, shake well. Detection conditions: Column: ACQUITY UPLCTMBEH C18 (1.7 μm, 50 mm * 2.1 mm); Column temperature: 35°C; Mobile phase: A 0.1% formic acid water (positive ion mode)/water, B acetonitrile; Flow rate: 0.2 Lmin; Injection volume: 5 μL; Autosampler temperature/TEM: 15°C.

Western Blot

Samples were cracked in RIPA lysis buffer plus PMSF in low temperature, and BCA assay kit (Santa Cruz, California, USA) detected total protein concentration. Prepared protein samples were separated in SDS-PAGE and transferred into 0.22 μm PVDF membranes and incubated with prepared antibodies. Finally, enhanced chemiluminescence (ECL, ThermoFisher, MA, USA) visualized this membrane. Antibodies against FOXO/p-FOXO and GAPDH were purchased from Abcam (Cambridge, MA, USA). Antibodies against MuRF-1, Atg5, Beclin-1, LC3I and LC3II were purchased from Proteintech Group (Proteintech Group, Wuhan, China).

H&E Staining

Pretibial muscle tissue was dissected from each group. The prepared muscle tissue slices were dewaxed and hydrated. After washed by water, synovial tissue slices were staining in hematoxylin solution for 5 min. Next, differentiated by 1% hydrochloric alcohol for 15s, the slices were washed with water. And then synovial tissue slices were stained by eosin solution for 1 min. Finally, muscle tissue slices were dehydrated, transparentized and sealed by neutral gum, observed under an optical microscope (Olympus, Tokyo, Japan).

Immunohistochemistry Staining

Pretibial muscle tissues were dissected from each group. First, Pretibial muscle tissue was fixed in 4% formaldehyde, embedded in paraffin. Each paraffin block was cut into 5 mm sections with a cryostat. The prepared Pretibial muscle tissue slices were dewaxed and hydrated followed washed by water. Secondly, Pretibial muscle tissue slices were sealed in 5 % normal goat serum for 30 min at room temperature. And then the slices were incubated with primary (p-FOXO 1:60, FOXO 1:300, LC3 1:300, Atg5 1:150, Beclin-1 1:100) antibody overnight at 4°C. After washing with PBS, the slices were incubated with biotinylated goat anti-rabbit IgG for 1 h. Finally, the slices were stained by DAB until a color change, and was observed under microscope (Olympus, Tokyo, Japan).

Masson Staining

Collect the tibial anterior muscle tissue, take out all the tissues, and dehydrate them sequentially through a layer of ethanol in a dehydrator. Put the melted paraffin into the embedding frame, place it on a -20°C freezer to cool, take it out of the embedding frame after the wax block solidifies and trim it, and place the embedded paraffin block in a 4°C refrigerator for setting. Slice after setting for 10 h. Briefly, Masson staining was performed on a 10 μm cryosection of muscle fixed with 95% alcohol for 20 min. Sections then were incubated with different solutions supplemented in Masson's Trichrome Stain Kit. At the end, the section was dehydrated with 95% alcohol for 10 sec, two rinses in anhydrous alcohol for 10 sec, and two rinses in xylene for 1 min each. The sections were mounted with Neutral balsam for imaging and fibrosis quantification. Muscle fibrosis quantification was performed by using Image J.

Transmissive Electron Microscope

Take rat tibial anterior muscle tissue, wash it with normal saline, immediately put it in a pre-chilled 2.5% glutaraldehyde solution, and fix it overnight at 4°C. After all tissues were fixed, the rat tibial anterior muscle tissue was cut into tissue blocks of 1 mm^3 size. Replace the 1% osmium acid solution, let it stand at 4°C for 2 h, and wash 3 times again with 1 x PBS. The tissue samples to be inspected were subjected to 50% (15 min), 70% (15 min), 80% (15 min), 90% (15 min), 95% (15 min), 100% (20 min), 100% (20 min) ethanol layer dehydration. After the transition of propylene oxide permeation, the samples were embedded with resin, and ultra-thin sections (thickness 70-90 nm) of lead citrate solution and 50% ethanol saturated solution of dioxy uranium acetate were stained for 15 min respectively. Under transmission electron microscope, images were collected to observe the ultrastructure of tissue samples.

Data Processing and Statistical Methods

The data obtained from the experiment were expressed by mean ± standard error (Mean ± SEM), and all data were processed and statistically analyzed using GraphPad Prism 6. The t-test was used for the comparison between the mean values of the two groups of samples, and the ANOVA test was used for the comparison between the mean values of multiple groups of samples. $P<0.05$ indicates that the difference is statistically significant.

Results

The Ingredients Contained in BYHWD

In order to study the main components of BYHW Decoction, HPLC and LC-MS were used to detect the contents of Isoflavones, Ferulic Acid, Paeoniflorin, Ligustrazine and Astragaloside in the medicinal solution, respectively. The analysis results showed that, the content of Astragaloside in the decoction (3.78 mg/mL) *(Fig. 1-A)* is much larger than that of other components,

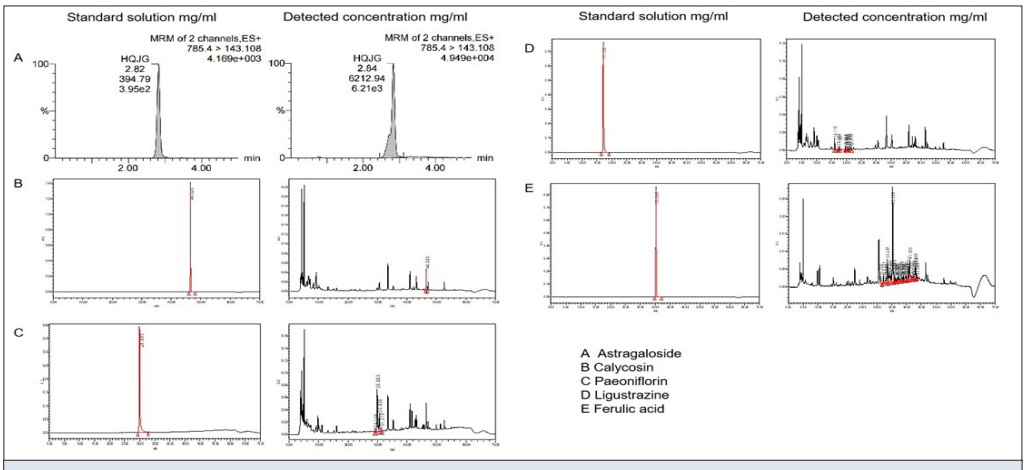


Fig 1. The concentration of the main components in BYHWD. **A**- The concentration of astragaloside; **B**- The concentration of calycosin; **C**- The concentration of paeoniflorin; **D**- The concentration of ligustrazine; **E**- The concentration of ferulic acid

Isoflavone (0.11 mg/mL) *(Fig. 1-B)*, Ferulic Acid (0.14 mg/mL) *(Fig. 1-C)*, Paeoniflorin (1.48 mg/mL) *(Fig. 1-D)*, Ligustrazine (0.0063 mg/mL) *(Fig. 1-E)*. The experimental results clearly indicate that astragaloside is the dominant chemical substance that dissolves after the BYHW decoction is boiled, suggesting that it may be one of the key substances underlying the efficacy of this compound formula. This also reflects the significant role of astragalus as the principal herb in the formula.

Astragaloside Inhibits the Atrophy Level of Skeletal Muscle After Nerve Injury

After determining the concentration of each component, we tested the therapeutic effect of each component on de-neuromuscular atrophy using mecobalamine tablets as positive control in animal models. HE staining results showed that compared with control group, muscle tissue of each treatment group was damaged to varying degrees, On the other hand, the degree of muscle tissue loss was significantly reduced in the treatment group compared with the blank model group *(Fig. 2-A)*. Except for the positive control of mecobalamine, Astragaloside group was the closest to normal tissues in terms of tissue morphology. The electron microscopy results of muscle tissue were similar to those of HE *(Fig. 2-B)*, which indicates that Astragaloside may be the main pharmacodynamic component.

Autophagy Plays an Important Role in Skeletal Muscle Denervation Atrophy

Based on previous studies on skeletal muscle, the ubiquitin-proteasome pathway or the autophagic lysosome pathway is the most likely deep cause of skeletal muscle denervati on atrophy. To this end, we examined and compared the expression levels of key proteins of these two signaling pathways in normal tissues and model tissues *(Fig. 2-C)*. As shown in *Fig. 2-C*, the expression level of LC3II/I and the ratio of LC3II/I in the model group were both increased, indicating the improved autophagy level of muscle cells. During autophagy formation, cytoplasmic type LC3 (LC3-I) will enzymolysis a small section of polypeptide and transform into membrane type (LC3-II). The increase of LC3-II represents the initiation of autophagy, and the LC3-II/I ratio can also estimate the level of autophagy. These results suggests that autophagy is the underlying cause of denervation atrophy in skeletal muscle.

Astragaloside Fights Skeletal Muscle Denervation by Inhibiting Muscle Autophagy

To verify this hypothesis, we treated animal model with Astragaloside alone, with autophagy labeled protein FOXO agonist as a control. The experimental results showed that the muscle dry-wet ratio in the model group was significantly improved after receiving Astragaloside treatment, but the data of group E was significantly decreased after the using of FOXO agonist *(Fig. 3-A,B,C)*, suggesting that the using of autophagy agonist could inhibit the therapeutic effect of Astragaloside on skeletal muscle denervation. Masson staining showed that the blue collagen fiber tissue of Astragaloside group was significantly less than that of model group, and the blue area of FOXO agonist group showed obvious expansion *(Fig. 3-D)*. Under electron microscope *(Fig. 3-E)*, the number of scattered autophagosomes in Astragaloside group was significantly reduced, but the number of autophagosomes was significantly increased after the use of FOXO agonist.

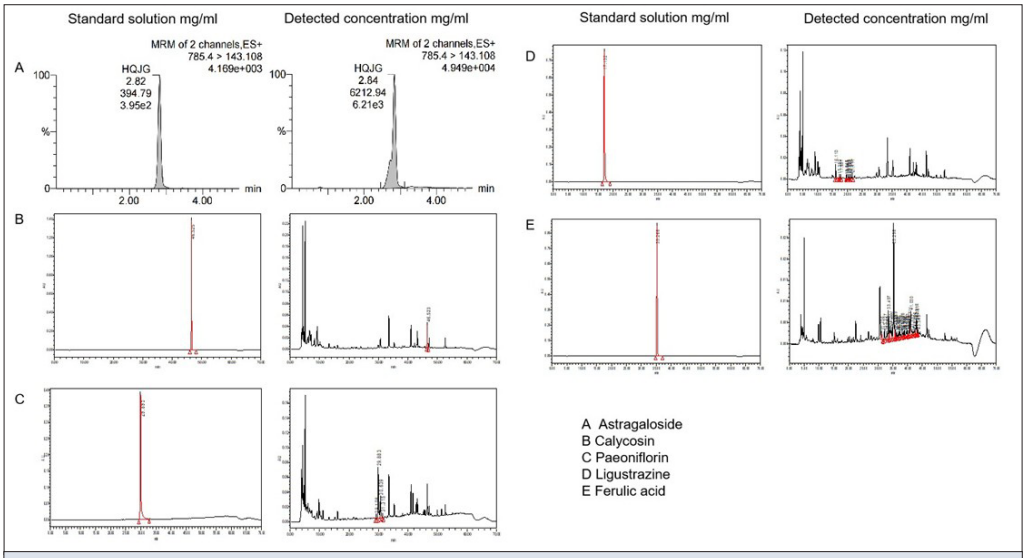


Fig 2. Therapeutic effects of each monomeric component on skeletal muscle atrophy. **A**-H&E staining results of muscle tissues after treatment in each group; **B**- Electron microscopic images of muscle tissue in each group after treatment; **C**- Expression levels of key proteins in muscular atrophy related signaling pathways (M: Model) (**P<0.01, ***P<0.001 vs. the control group

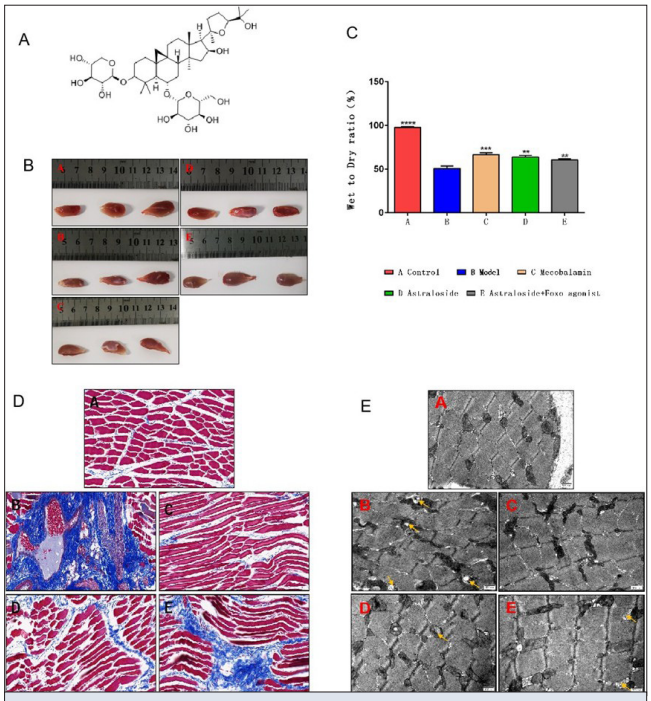


Fig 3. Terapeutic effects of Astragaloside on skeletal muscle nerve injury. **A**- The molecular structure of astragaloside; **B**- Morphology of tibial anterior muscle in each group after treatment: **C**- The ratio of dry weight and wet weight of anterior tibial muscle in each group after treatment; **D**- Masson staining of tibial anterior muscle in each group after treatment; **E**- Electron microscopic morphology of tibial anterior muscle in each group after treatment. *Yellow arrows:* Autophagosome. *P<0.05, **P<0.01, ***P<0.001 vs. the control group

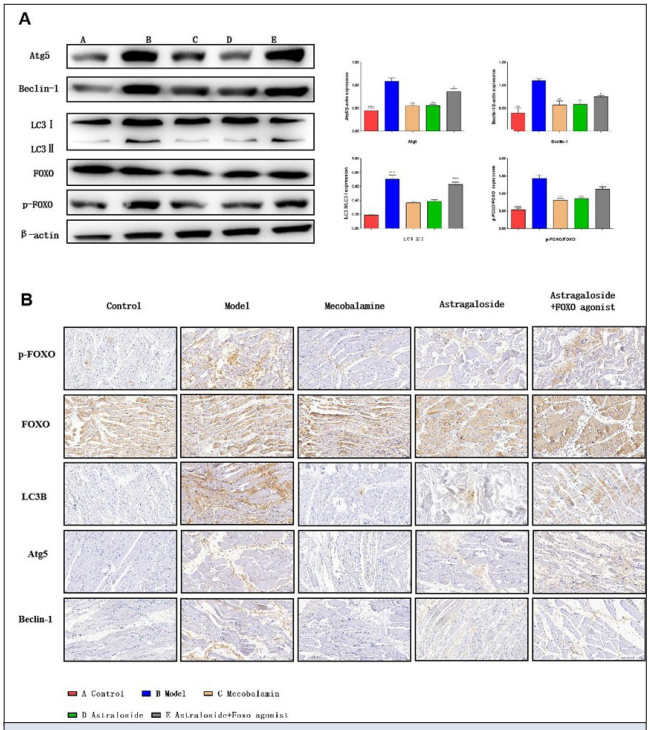


Fig 4. Astragaloside regulates autophagy in skeletal muscle cells through autophagy related pathway. **A**- Western Blot results of autophagy-related proteins in tibial anterior muscle after treatment; **B**- Immunohistochemical results of autophagy-related proteins in tibial anterior muscle after treatment. *P<0.05, **P<0.01, ***P<0.001 vs. the control group

These results suggest that Astragaloside inhibits skeletal muscle denervation via lysosomal autophagy.

Astragaloside Inhibits Skeletal Muscle Denervation Autophagy Through FOXO Related Pathway

Autophagy is a highly conserved and multi-step metabolic process that maintains homeostasis of the intracellular environment by degrading damaged proteins, cellular metabolites and diseased organelles. The occurrence and development of many diseases are associated with changes in autophagy activity, and the autophagy related gene microtubule-associated protein 1 light chain 3, LC3 and autophagy related gene-5 (ATG5) are both important genes involved in the regulation of autophagy activity. In our results, the expression level of LC3 and Atg5 protein were significantly upregulated after animal model was established and down-regulated after treatment which indicates us the important role of autophagy in skeletal muscle denervation atrophy *(Fig. 4-A,B)*. Besides, studies have shown that FOXO can activate the autophagy mechanism of different cell types by affecting the expression of autophagy genes which including ATG5. Therefore, we used FOXO agonists as a distraction to determine whether autophagy in muscle tissue after motor nerve injury is mediated by changes in the FOXO pathway. As predicted, the addition of FOXO agonists reversed the efficacy of the treatment in both the mecobalamine and astragaloside groups.

Discussion

In this study, starting from the basic composition of traditional Chinese medicine, the contents of the five most important components in the BYHWD, Isoflavones, Ferulic acid, Paeoniflorin, Ligustrazine and Astragaloside, were detected by HPLC and LC-MS methods [8]. All monomers have a certain inhibitory effect on skeletal muscle atrophy caused by nerve injury in vivo. Among them, Astragaloside has the highest concentration in decoction, and its monomer has the most obvious inhibitory effect on muscle atrophy [9]. Pharmacologically speaking, Astragaloside has many pharmacological activities, it can effectively activate mononuclear macrophage system, stimulate macrophage and T cell function to play an antiviral effect; Astragaloside can prevent adrenal hyperplasia and thymus atrophy in the alert phase of stress response, and prevent abnormal changes in the resistance phase and exhaustion phase of stress response so as to play an anti-stress role [10]. In addition, Astragaloside can also enhance cell metabolism, promote blood circulation, and improve cardiopulmonary function in some cases [11].

In terms of clinical research, Astragaloside has a good

curative effect in the treatment of the body after nerve injury. Qi et al.[12] used BYHWD to feed rats after spinal cord injury. The experimental results show that the decoction can inhibit PAF. The application of BYHW significantly improved the motor function of rats; the research results of Zhao et al.[13] team on the gerbil model of ischemia-reperfusion injury showed that BYHWD could protect the nerve function of gerbils after reperfusion injury by improving brain microcirculation. A study indicated that BYHWD can inhibit the apoptosis of nerve cells caused by hypoxia by eliminating reactive oxygen species and NO [14]. Our results show that the inhibitory effect of BYHWD on skeletal muscle denervation may be produced by inhibiting skeletal muscle cell autophagy.

Whether it is the expression of autophagy-related proteins after monomer treatment, or the immunohistochemical results of autophagy-related proteins in tissues, and the number of autophagy corpuscles in tissues under electron microscopy, the results of autophagy-related detection showed significant changes among the groups [15]. This also directly affects the wet-to-weight ratio and cross-sectional area of skeletal muscle after treatment. Autophagy is a dynamic process through which cytoplasmic components can be decomposed into basal components and then re-entered into the cytoplasm for reuse [16]. Autophagy is also a major protective mechanism that allows cells to survive a variety of stress conditions, such as nutrient or growth factor deprivation, hypoxia, reactive oxygen species (ROS), DNA damage, and more [17]. MuRF-1 encodes E3s ubiquitin ligase, which is essential for protein ubiquitination degradation and determines the degradation rate of this pathway [18]. However, from the detection results of samples, there was no significant difference in the expression of MuRF-1 in normal tissue and model group, but there was significant difference in the expression of LC3, the signature protein of the autophagic lysosome pathway [17]. Under basic conditions, low levels of autophagy exist in all types of cells, but stimuli such as nutritional deficiencies or hypoxia may lead to up-regulation of autophagy levels [19].

After the injury of the common peroneal nerve, the conduction of nerve impulses is hindered, resulting in the disuse of some muscle fibers controlled downstream, resulting in disuse muscular atrophy [20]. At the same time, the release of acetylcholine from the peripheral parts of the damaged nerve fibers decreases, and sympathetic nerve nutrition weakens, resulting in muscle atrophy [21]. Our findings reveal a possible mechanism of muscle disuse atrophy, that is, after motor nerve injury, downstream skeletal muscle due to lack of nutritional factors in order to maintain mixing, the level of autophagy in skeletal muscle cells increases, and the number of muscle fibers decreases, resulting in muscle atrophy. Combined with the research results of Cheng et al.[22], on the one hand, BYHWD strengthened the microcirculation downstream of injury and alleviated the lack of nutritional factors caused by nerve injury, on the other hand, its main component, Astragaloside, can effectively reduce the expression of autophagy related proteins in skeletal muscle, thereby inhibiting skeletal muscle atrophy.

Motor nerve injury induces muscle atrophy via autophagy activation and nutrient deficiency. BYHWD alleviates atrophy by improving microcirculation and its component Astragaloside suppresses autophagy, offering a therapeutic strategy for nerve injury-related muscle wasting.

Declarations

Data Availability Statement: All processed data and models used during the study are available from the corresponding author (HW) by request.

Acknowledgments: We would like to thank all the researchers and study participants for their contributions.

Funding Support: This study was supported by The General project of Natural Science Foundation of Jiangsu Province (Grant No. BK20201399).

Ethical Approval

All procedures performed in the studies involving animals were in accordance with the ethical standards of the Institutional Animal Care and Use Committee (IACUC) of Nanjing University of Chinese Medicine (No. 202203A041).

Declaration of Conflicting Interests: The author(s) declared no potential conflicts of interest.

Declaration of Generative Artificial Intelligence: We declare that the ariticle and tables/figures are not written by AI.

Authors' Contribution: L.Z. and HW: fully responsible for the study designing, Research fields, Drafting, Finalizing the paper; S.L., L.M., and G.W.: Wrote the manuscript and drew the pictures, Collected and organize literature; H.W. and L.Z.: Proofread the manuscript. All authors have reviewed and agreed to the published version of the manuscript.

Reference

1. Cohen S, Nathan JA, Goldberg AL: Muscle wasting in disease: Molecular mechanisms and promising therapies. *Nat Rev Drug Discov,* 14 (1): 58-74, 2015. DOI: 10.1038/nrd4467

2. Baehr LM, Hughes DC, Waddell DS, Bodine SC: SnapShot: Skeletal muscle atrophy. *Cell,* 185 (9):1618-1618.e1, 2022. DOI: 10.1016/j.cell.2022.03.028

3. Braun TP, Zhu X, Szumowski M, Scott GD, Grossberg AJ, Levasseur PR, Graham K, Khan S, Damaraju S, Colmers WF, Baracos VE, Marks DL: Central nervous system inflammation induces muscle atrophy via activation of the hypothalamic-pituitary-adrenal axis. *J Exp Med,* 208 (12): 2449-2463, 2011. DOI: 10.1084/jem.20111020

4. Derde S, Hermans G, Derese I, Güiza F, Hedström Y, Wouters PJ, Bruyninckx F, D'Hoore A, Larsson L, Van den Berghe G, Vanhorebeek I: Muscle atrophy and preferential loss of myosin in prolonged critically ill patients. *Crit Care Med,* 40 (1): 79-89, 2012. DOI: 10.1097/CCM.0b013e31822d7c18

5. Faruk MO, Ichimura Y, Komatsu M: Selective autophagy. *Cancer Sci,* 112

(10): 3972-3978, 2021. DOI: 10.1111/cas.15112

6. Fu Y, Cai J, Xi M, He Y, Zhao Y, Zheng Y, Zhang Y, Xi J, He Y: Neuroprotection effect of astragaloside IV from 2-DG-induced endoplasmic reticulum stress. *Oxid Med Cell Longev,* 2020:9782062, 2020. DOI: 10.1155/2020/9782062

7. Wang H, He Y, Wan L, Li C, Li Z, Li Z, Xu H, Tu C: Deep learning models in classifying primary bone tumors and bone infections based on radiographs. *npj Precis Onc,* 9:72, 2025. DOI: 10.1038/s41698-025-00855-3

8. Peng J, Ge C, Shang K, Liu S, Jiang Y: Comprehensive profiling of the chemical constituents in Dayuanyin decoction using UPLC-QTOF-MS combined with molecular networking. *Pharm Biol,* 62 (1): 480-498, 2024. DOI:10.1080/13880209.2024.2354341

9. Glick D, Barth S, Macleod KF: Autophagy: cellular and molecular mechanisms. *J Pathol,* 221 (1): 3-12, 2010. DOI: 10.1002/path.2697

10. Lattouf NA, Tomb R, Assi A, Maynard L, Mesure S: Eccentric training effects for patients with post-stroke hemiparesis on strength and speed gait: A randomized controlled trial. *NeuroRehabilitation,* 48 (4): 513-522, 2021. DOI:10.3233/NRE-201601

11. Li C, Zhang Y, Liu J, Kang R, Klionsky DJ, Tang D: Mitochondrial DNA stress triggers autophagy-dependent ferroptotic death. *Autophagy,* 17 (4): 948-960, 2021. DOI: 10.1080/15548627.2020.1739447

12. Qi YN, Tan MS, Wang YL, Wang W, Wu XJ, Hao QY, Yi P, Yang F, Tang XS: Effect of Buyanghuanwu decoction on the expression of platelet activating factor after acute spinal cord injury in rats. *Zhongguo Gu Shang,* 31 (2): 170-174, 2018. DOI: 10.3969/j.issn.1003-0034.2018.02.015

13. Zhao YN, Wu XG, Li JM, Chen CX, Rao YZ, Li SX: Effect of BuYangHuanWu recipe on cerebral microcirculation in gerbils with ischemia-reperfusion. *Sichuan Da Xue Xue Bao Yi Xue Ban,* 41 (1): 53-56, 2010.

14. Rodriguez-Aller M, Gurny R, Veuthey JL, Guillarme D: Coupling ultra high-pressure liquid chromatography with mass spectrometry: Constraints and possible applications. *J Chromatogr A,* 1292, 2-18, 2013. DOI: 10.1016/j.chroma.2012.09.061

15. Shi H, Zhou P, Gao G, Liu PP, Wang SS, Song R, Zou YY, Yin G, Wang L: Astragaloside IV prevents acute myocardial infarction by inhibiting the TLR4/MyD88/NF-κB signaling pathway. *J Food Biochem,* 45 (7):e13757, 2021. DOI: 10.1111/jfbc.13757

16. Urbańska K, Orzechowski A: The secrets of alternative autophagy. *Cells,* 10 (11):3241, 2021. DOI: 10.3390/cells10113241

17. Wang C, Haas M, Yeo SK, Sebti S, Fernández ÁF, Zou Z, Levine B, Guan JL: Enhanced autophagy in Becn1F121A/F121A knockin mice counteracts aging-related neural stem cell exhaustion and dysfunction. *Autophagy,* 18 (2): 409-422, 2022. DOI: 10.1080/15548627.2021.1936358

18. Wang F, Zhao Y, Chen S, Chen L, Sun L, Cao M, Li C, Zhou X: Astragaloside IV alleviates ammonia-induced apoptosis and oxidative stress in bovine mammary epithelial cells. *Int J Mol Sci,* 20 (3):600, 2019. DOI: 10.3390/ijms20030600

19. Yang Z, Lin P, Chen B, Zhang X, Xiao W, Wu S, Huang C, Feng D, Zhang W, Zhang J: Autophagy alleviates hypoxia-induced blood-brain barrier injury via regulation of CLDN5 (claudin 5). *Autophagy,* 17 (10): 3048-3067, 2021. DOI: 10.1080/15548627.2020.1851897

20. Zhang M, Yi Y, Gao BH, Su HF, Bao YO, Shi XM, Wang HD, Li FD, Ye M, Qiao X: Functional characterization and protein engineering of a triterpene 3-/6-/2'-O-glycosyltransferase reveal a conserved residue critical for the regiospecificity. *Angew Chem Int Ed Engl,* 61:e202113587, 2022. DOI: 10.1002/anie.202113587

21. Zhang ZQ, Song JY, Jia YQ, Zhang YK: Buyanghuanwu decoction promotes angiogenesis after cerebral ischemia/reperfusion injury: Mechanisms of brain tissue repair. *Neural Regen Res,* 11 (3): 435-440, 2016. DOI: 10.4103/1673-5374.179055

22. Cheng M, Li T, Hu E, Yan Q, Li H, Wang Y, Luo J, Tang T: A novel strategy of integrating network pharmacology and transcriptome reveals

antiapoptotic mechanisms of Buyang Huanwu Decoction in treating intracerebral hemorrhage. *J Ethnopharmacol,* 319 (Pt 1):117123, 2024. DOI: 10.1016/j.jep.2023.117123